Available online at www.sciencedirect.com

ScienceDirect

Geochimica et Cosmochimica Acta 188 (2016) 58–72

Geochimica et Cosmochimica Acta

www.elsevier.com/locate/gca

Analysis of the site-specific carbon isotope composition of propane by gas source isotope ratio mass spectrometer

Alison Piasecki [a,*], Alex Sessions [a], Michael Lawson [b], A.A. Ferreira [c], E.V. Santos Neto [c], John M. Eiler [a]

[a] Division of Geological and Planetary Sciences, California Institute of Technology, Pasadena, CA 91125, United States
[b] Exxon Mobil Upstream Research Company, Science 1, 2A.513, 22777 Springwoods Village Parkway, Spring, TX 77389, United States
[c] Division of Geochemistry, PETROBRAS Research and Development Center (CENPES), PETROBRAS, Rua Horácio Macedo, 950, Ilha do Funadão, Rio de Janeiro, RJ 21941-915, Brazil

Received 4 September 2015; accepted in revised form 29 April 2016; Available online 26 May 2016

Abstract

Site-specific isotope ratio measurements potentially provide valuable information about the formation and degradation of complex molecules—information that is lost in conventional bulk isotopic measurements. Here we discuss the background and possible applications of such measurements, and present a technique for studying the site-specific carbon isotope composition of propane at natural abundance based on mass spectrometric analysis of the intact propane molecule and its fragment ions. We demonstrate the feasibility of this approach through measurements of mixtures of natural propane and propane synthesized with site-specific ^{13}C enrichment, and we document the limits of precision of our technique. We show that mass balance calculations of the bulk $\delta^{13}C$ of propane based on our site-specific measurements is generally consistent with independent constraints on bulk $\delta^{13}C$. We further demonstrate the accuracy of the technique, and illustrate one of its simpler applications by documenting the site-specific carbon isotope signature associated with gas phase diffusion of propane, confirming that our measurements conform to the predictions of the kinetic theory of gases. This method can be applied to propane samples of moderate size (tens of micromoles) isolated from natural gases. Thus, it provides a means of studying the site-specific stable isotope systematics of propane at natural isotope abundances on sample sizes that are readily recovered from many natural environments. This method may also serve as a model for future techniques that apply high-resolution mass spectrometry to study the site-specific isotopic distributions of larger organic molecules, with potential applications to biosynthesis, forensics and other geochemical subjects.

Keywords: Stable isotopes; Site-specific isotopes; Natural gas; Mass spectrometry

1. INTRODUCTION

Abundances of stable isotopes are widely used to constrain problems in the natural and applied sciences; e.g., paleothermometry, geochemical budgets, and forensic identification (Lamprecht and Pichlmayer, 1994; Snell et al., 2014). Such work often focuses on the stable isotopes of light elements (D, ^{13}C, ^{15}N, ^{18}O, etc.), measured using gas source isotope ratio mass spectrometry (IRMS). These techniques generally require that samples be chemically converted to the appropriate analyte gases (H_2, N_2, CO_2); a common example is carbon isotope analysis of organic matter, which is accomplished by oxidation to yield CO_2 that is then analyzed by mass spectrometry for its $^{13}CO_2/^{12}CO_2$ ratio.

Such measurements constrain the isotopic content for that analyte, averaged over all elemental positions within

* Corresponding author.
E-mail address: piasecki@gps.caltech.edu (A. Piasecki).

http://dx.doi.org/10.1016/j.gca.2016.04.048
0016-7037/

its molecular structure. However, this approach obscures intramolecular variations in isotopic content. For example, there is evidence that adjacent carbon positions within fatty and amino acids can differ from one another in $\delta^{13}C$ by up to ~30‰ (Abelson and Hoering, 1961; DeNiro and Epstein, 1977; Monson and Hayes, 1980). Such differences reflect isotope effects associated with biosynthetic pathways, and potentially serve as forensic identifiers and/or records of metabolic strategy, environmental conditions, stress, and perhaps other information. Theoretical studies of the isotope structures of organic molecules in thermodynamically equilibrated populations of molecules suggest the possibility of geothermometers based on site-specific differences in $\delta^{13}C$, δ D and perhaps other elements (Rustad, 2009; Webb and Miller, 2014; Piasecki et al., 2015). Large, structurally complex molecules presumably record a number of equilibrium and kinetic processes in their isotopic anatomies, perhaps 'fingerprinting' their biosynthetic (or geochemical) origins, processes and pathways involved in their modification or degradation, as well as local environmental variables like temperature, or potentially even more obscure environmental variables like humidity and oxidation state. Whatever these intramolecular variations might record, analytical techniques that yield bulk isotopic content obviously result in the loss of information. Larger organic molecules suffer the most from these techniques. Similarly, conventional methods based on chemical conversion of analytes to H_2 or CO_2 also destroy any information that might be recorded by the abundances of multiply substituted (or 'clumped') isotopologues.

A variety of methods have been developed to observe intramolecular isotopic distributions, including position-specific and multiple substitutions. 'Clumping' or multiple substitution, has been studied in several molecules, including (but not limited to) CO_2, ethane, N_2O, O_2 and methane (Schauble et al., 2006; Magyar et al., 2012; Clog et al., 2013; Stolper et al., 2014a,b; Yeung et al., 2014; Stolper et al., 2015). These measurements have been enabled by innovations in isotope ratio mass spectrometry, including detector arrays configured with high-sensitivity detectors for quantification of the low-intensity multiply-substituted ion beams, and a prototype instrument with a high-resolution, double-focusing analyzer capable of mass resolving isobaric interferences such as $^{13}CH_4$ vs. $^{12}CH_3D$ or $^{15}N^{14}N^{16}O$ vs. $^{14}N_2{}^{17}O$. (Note that some measurements of this kind may also be possible using IR absorption spectroscopy (Ono et al., 2014)).

Measurements of site-specific isotopic substitutions have been attempted using several approaches; the earliest work of this kind used chemical techniques to isolate carbon from specific moieties from organic compounds. For example, Abelson and Hoering (1961) decarboxylated amino acids to measure the $\delta^{13}C$ of their COOH groups (Abelson and Hoering, 1961; Macko et al., 1987), and Monson and Hayes degraded fatty acids with a combination of ozonolysis and decarboxylation to analyze the site-specific ordering of ^{13}C (Monson and Hayes, 1980, 1982). NMR is inherently a site-specific technique for measuring isotopes that has been used to study of both ^{13}C and D within organic molecules (Moussa et al., 1990; Caer et al., 1991; Caytan et al., 2007). Advancements in the sensitivity and stability of NMR have led to 'SNIF-NMR' techniques that determine natural abundances of stable isotopes in organic structures (Martin et al., 1986; Singleton and Szymanski, 1999). These techniques are – thus far – capable of observing only singly-substituted isotopologues and require large sample sizes (100's of mg's), but have proven effective at recognizing even subtle (per mil level) differences among sugars, alkanes and other compounds (Gilbert et al., 2013). Isotope ratio mass spectrometry has been used to measure site-specific ^{15}N distributions in N_2O, based on comparison of the ^{15}N content of the N_2O^+ molecular ion and the NO^+ fragment ion (Toyoda and Yoshida, 1999; Westley et al., 2007). Finally, IR absorption spectroscopy techniques have proven capable of precisely measuring site-specific ^{15}N distribution in N_2O (Uehara et al., 2003).

Here we extend the concepts behind the mass spectrometric analysis of site-specific isotopic compositions of N_2O to the problem of ^{13}C distributions in organic matter, using a high-resolution IRMS instrument, the Thermo 253 Ultra, to mass resolve isobaric interferences that commonly occur in the mass spectra of hydrocarbons (Eiler et al., 2013). We focus on propane, which is among the smallest and simplest organic molecules that could record site-specific carbon isotope variations. And, there are reasons to believe such differences could give rise to useful geochemical tools: most natural propane is derived from thermal degradation ('cracking') of components of kerogen or liquid hydrocarbons, which itself derives from catagenesis of biosynthetic compounds, like fatty acids, that are known to possess intramolecular carbon isotope variations (DeNiro and Epstein, 1977; Monson and Hayes, 1980, 1982). Thus, propane could inherit an isotopic structure from its precursors, and/or record the mechanisms and conditions of cracking reactions. In addition, propane is destroyed in natural environments through thermal degradation, biological consumption, and atmospheric photo-oxidation, (Clayton, 1991; Berner et al., 1995; Takenaka et al., 1995; Hinrichs et al., 2006) all of which could impart a distinctive signature on the site-specific carbon isotope content of residual propane.

This paper describes the methods of a new mass spectrometric technique for site-specific carbon isotope analysis of propane, examples of its use on products of simple experiments and propane isolated from natural gas, and a discussion of its possible uses in wider applications. A companion paper to follow will build on this base with data for a variety of natural and synthetic gases, as well as a broader discussion of the expected systematics of site-specific carbon isotope composition of propane generated by thermal degradation of buried organic matter.

2. SAMPLE PREPARATION

2.1. Sample purification

The mass spectrometric method we present calls for a typical sample size of ~50 μmol of purified propane (less is possible, but this quantity assures adequate source

pressure over the course of several measurements each of several molecular fragments). Sample preparation typically involves separation from other gases, particularly in the case of natural gases, where propane is generally a minor component ($\leqslant\sim$5%). We perform this purification via cryogenic distillation. Although alternate methods, such as preparatory gas chromatography, may be equally or more effective, this approach was chosen because it is easily used for a wide range of sample size and purity, and can be combined with methods for separation of related analytes (methane, ethane, etc.).

A sample gas aliquot containing at least ~50 μmol propane is introduced into a glass vacuum line that contains, in addition to various cryogenic traps and calibrated volumes, a liquid-helium-cooled cryostat. The aliquot of sample gas is first exposed to the cryostat at 20 K, which condenses propane along with ethane, methane and other species such as CO_2 and N_2. The remaining vapor, consisting of highly non-condensable gases like He and H_2, is pumped away. Next, methane is removed from the sample gas mixture as previously described in (Stolper et al., 2014b): We repeatedly cycle the cryostat between 80 K and 45 K in order to release N_2 while retaining CH_4 (Stolper et al., 2014b). The cryostat is then raised to 72 K and methane is released and trapped on a molecular sieve held at liquid N_2 temperature, and removed from the vacuum line for isotopic analysis (Stolper et al., 2014b).

Next, a similar process is used to isolate ethane and propane. The temperature is raised to 135 K for 5 min, and then lowered to 115 K with the valve to the cryostat closed. It is then opened and exposed to a trap immersed in liquid nitrogen, into which ethane condenses. The cryostat is re-closed, and the temperature is raised to 150 K for 5 min and then lowered to 135 K. The propane is then exposed to and condenses in a trap immersed in liquid nitrogen, separating it from higher-order hydrocarbons like butane. The cryostat is then closed again, the temperature raised to 150 K, and then the cryostat is re-opened and the residual gas is pumped away. The cryostat is then lowered to 60 K, the ethane is frozen into it, and the processes are repeated, each time adding the propane fraction to the previously separated propane. This process is repeated 5 times, or until the pressure on the ethane and propane fractions does not change between cycles.

A further complication arises when CO_2 is present in a sample, because CO_2 has a similar vapor pressure to propane. We separate CO_2 from otherwise purified propane by passing the gas released between 135 K and 150 K (above) over ascarite multiple times, until its pressure does not significantly change with further ascarite exposure.

A series of tests were conducted to verify purification techniques. Propane and ethane were mixed together and run through the purification technique in approximately equal aliquots on the glass line. The recovery of propane and ethane was nearly complete (97%). Although there was not 100% purification, comparison of the isotopic composition of the propane purified from a propane/ethane mixture to a pure aliquot of that same propane showed the ethane/propane separation process neither fractionates the isotopes of propane nor compromises the analysis of propane due to trace ethane contamination. We verified that the CO_2 removal step does not fractionate or otherwise compromise isotopic analysis of in a similar fashion: we prepared a mixture that was 3 parts propane to 1 part CO_2. After exposure to ascarite, we recovered a quantity of propane consistent with a 100.8% yield, and found its isotopic composition was indistinguishable from the starting propane. Based on these results, we conclude that our procedures for separating propane from ethane and CO_2 are both reproducible and quantitative.

Subsequent to performing the work presented in this paper, we have added a further purification procedure involving separation of propane from higher order hydrocarbons (mostly butane and pentane) by gas chromatography over a room-temperature packed column of ShinCarbon. This procedure is not necessary to obtain propane sufficiently pure for analysis, but improves the consistency of the purity of propane extracted from relatively wet natural gases, and therefore reduces the rate of failures of our procedure arising from contaminants (below). We recommend this modification to anyone adopting the techniques described above.

2.2. Contaminant characterization

The cryogenic purification procedure outlined above for propane can fail to remove trace amounts of propene, butane, and pentane, which have small but significant vapor pressures at 150 K. Evidence of these contaminants can be found by conducting a mass scan on purified propane samples, looking for diagnostic departures from the mass spectrum of pure propane; this test is made on all unknown samples isolated from natural gas. We also measure ratios of intensities of several characteristic masses and compare them to those ratios for pure propane from our reference tank measured under the same instrument tuning conditions as the unknown sample, again to recognize evidence of contaminants and calculate their contributions to masses of interest. For example, the intensity ratio of masses 57 and 58 constrains the abundance and speciation of butane contamination; if there is negligible mass 57 or 58 signal, then we conclude that there is no butane contamination. Conversely, if masses 57 and 58 are present and 58/57 <1 then butane is present and dominated by a *n*-butane contaminant; if they are present and the ratio is greater than 1, then the contaminant is dominated by iso-butane.

Similar indices can also be used to recognize and approximately quantify contamination by CO_2, ethane, and propene. CO_2 and ethane are recognized by a combination of the mass 29/28 ratio (propane = 1.7, CO_2 = 0.01, ethane = 0.2), while propene is apparent in the mass 44/43 ratio (propane = 1.18, propene = 0.043). By assuming a linear relationship between the proportions of the suspected contaminants and their contributions to the mass spectrum (a simplifying approximation), the species present in the gas can be calculated, and further cryogenic separations are preformed until the contaminants are less than 1% of the highest intensity propane beam at mass 29. One failure of this approach is that we occasionally observe samples with significant excesses of methyl fragment ions

at 15 amu (i.e., this ion beam is present in significantly greater proportion than seen in a concurrently analyzed pure propane standard), and we have not yet established the contaminant species that is (or are) responsible for this difference. Therefore, in addition to discarding data on samples containing 1% or more of a recognized contaminant, we discard data for samples in which one or more diagnostic propane ion intensity ratios disagrees with that for a concurrently run pure propane standard by 7.5% or more (an empirically selected threshold, based on the observed mass spectra of samples that fail to match independent constraints on their bulk isotopic compositions). Note, the numbers listed above for propane are taken from the National Institute of Standards, but due to variations in ion source operating parameters they do not always match the measured value. Thus the 'correct' ratio for pure propane on any given day is based on a measurement of the reference gas standard (though the NIST value is generally within 1% of the measured reference value for each of the listed ratios).

Although we have evidence to suggest that our sample purification procedure can yield gases of sufficient purity for accurate analysis (see below), trace contaminants are often still present; we can generally detect ethane in propane purified from natural gas (though the latter is harder to detect because there is no mass range where there are ethane peaks and not propane peaks; i.e., it can only be recognized by changes in proportions of fragment ions). We have found no evidence for propene within any of the natural samples yet measured. CO_2 is common in most of the samples that have been analyzed so far, both conventional natural gas samples as well as shale gas samples. Even after multiple ascarite cleanup steps, trace CO_2 remains. However, these trace contaminants are generally below our 1% threshold, and data provided below indicates they do not lead to significant systematic errors in measured carbon isotope ratios.

3. MASS SPECTROMETRY

The goal of the analytical method that we present is to determine variations in the relative enrichment of ^{13}C between the terminal ('methyl') and central ('methylene') carbon positions of propane. The strategy that we employ combines two previously reported innovations: (1) Eiler et al. (2013) and Stolper et al. (2014) demonstrated that the recently developed Thermo IRMS 253 Ultra, a prototype high-resolution isotope ratio mass spectrometer, is capable of mass resolving isobaric interferences among ^{13}C- and D-bearing isotopologues and H-adducts of methane. We explore here whether this capability can be applied with useful precision to fragment ions generated by electron ionization (EI) of propane. And, (2) Toyoda and Yoshida (1999) demonstrate that comparison of the $^{15}N/^{14}N$ ratio of N_2O^+ and NO^+ ions generated by N_2O constrains the distribution of ^{15}N between the terminal and central N position. By analogy, we explore here whether comparison of the $^{13}C/^{12}C$ ratios of fragment and molecular ions of propane can constrain the distribution of ^{13}C between its central and terminal positions.

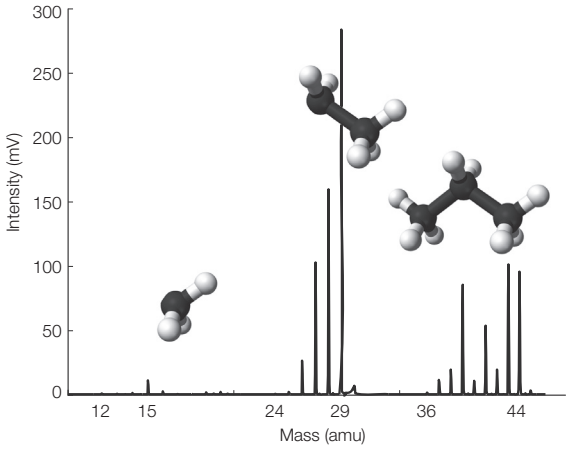

Fig. 1. Mass spectrum of propane from the MAT 253 Ultra, collected using a faraday cup registered through a $10^8\ \Omega$ amplifier. The structures of major fragment and molecular ions are illustrated with ball and stick figures.

Fig. 1 illustrates the low-resolution mass spectrum (i.e., only cardinal masses are shown) of propane under commonly used electron impact ion source conditions ($\sim 10^{-7}$ mbars pressure; 70 eV electron impact energies). The most abundant ion is $C_2H_5^+$, with a nominal mass of 29 Da. The adjacent peak at mass 30 consists of $^{13}C^{12}CH_5^+$ and lesser amounts of $^{12}C_2H_4D^+$ and $^{12}C_2H_6^+$ (as well as traces of other species, such as $^{13}C_2H_4^+$), and the family of peaks of descending abundance from 28 to 24 Da each is dominated by $^{12}C_2^+$ with 4, 3, 2, 1 or no hydrogens (plus small amounts of ^{13}C and D-bearing isotopologues and traces of multiply substituted species containing fewer hydrogens). This pattern is mirrored by less abundant but generally similar mass spectra for the CH_n^+ and $C_3H_n^+$ ionic species (masses 12–16 and 36–45, respectively). We use a shorthand for these families of peaks throughout the rest of this paper: the three-carbon species are referred to as the 'propyl fragments,' the two-carbon species as the 'ethyl fragments' and the one-carbon species as the 'methyl fragments.' Similarly, we refer to the terminal carbon positions of the parent molecule as the 'terminal' positions, methyl, or the 'C-1' and 'C-3' positions (the two are symmetrically equivalent), and the central carbon position as the 'center', 'methylene', or 'C-2' position.

Our analytical strategy relies on the high resolution of the Thermo IRMS 253 Ultra to measure the intensity ratios of ^{12}C and ^{13}C-bearing isotopologues of ions that share the same elemental stoichiometry, free from interferences by other species that share the same cardinal mass (Eiler et al., 2013). Following a method first developed for site-specific ^{15}N analysis of N_2O, we constrain the differences in ^{13}C content between the center and ends of propane by comparing the $^{13}C/^{12}C$ ratios of fragments that sample different proportions of these two sites. In particular, we constrain the $^{13}C/^{12}C$ ratio of the terminal carbon position by analyzing methyl fragment ions (under the assumption that, to first order, they will preferentially come from the terminal carbon positions). Because there are no fragments

that one might reasonably assume exclusively sample the center carbon, its isotopic composition must be constrained by difference. We do this via a separate measurement of the $^{13}C/^{12}C$ ratio of one of the ethyl fragments, which we assume mostly comprise the center carbon plus one terminal carbon. Given these assumptions (which we test experimentally below), the difference in $^{13}C/^{12}C$ ratio (^{13}R) between the center and terminal carbon position can be calculated approximately as:

$$\left[{}^{13}R_{methyl}\right] = {}^{13}R_{terminal} \quad (1)$$

$$\left[{}^{13}R_{ethyl}\right] = \frac{{}^{13}R_{center} + {}^{13}R_{terminal}}{2} \quad (2)$$

$$\left[{}^{13}R_{center}\right] = 2 \times {}^{13}R_{ethyl} - {}^{13}R_{methyl} \quad (3)$$

And the bulk $^{13}C/^{12}C$ ratio of the whole molecule can be calculated as:

$$\left[{}^{13}R_{propyl}\right] = \frac{1}{3}\left(2 \times {}^{13}R_{ethyl} + {}^{13}R_{methyl}\right) \quad (4)$$

In principle, under the assumptions behind Eqs. (1)–(4), it is possible to constrain $R_{terminal}$ and R_{center} by measuring any combination of two fragments: methyl and ethyl, methyl and propyl, or even ethyl and propyl fragments. We note that a conventional measurement of propane $\delta^{13}C$ could also substitute for measuring the propyl fragment. Moreover, each of the major groups of fragments (methyl, ethyl and propyl) exists as several homologs that differ in their numbers of hydrogens, any of which could be measured independently. (Though presumably measuring two or more species that share the same carbon number and differ only in hydrogen number would not add useful constraints, unless more complex source chemistry leads to differences between such species in the proportions of center and terminal carbons.) Measuring 3 or more fragments would over-constrain the problem, and provide an additional test for internal consistency. Thus, the measurement we explore here could be performed in a variety of ways, and the version we present should be thought of as a representative case.

There are three principal challenges to turning this conceptual approach into a precise and accurate analytical method:

We must be able to analyze both the ^{12}C and ^{13}C isotopologues of the two chosen fragments, resolved from closely adjacent isobaric interferences (e.g., $^{13}CH_3^+$ vs. $^{12}CH_2D^+$) and free from (or corrected for) other possible contaminant isobars.

We must rigorously understand how various fragment ions sample the two different carbon sites, e.g. whether the center carbon position contributes to methyl fragments in the mass spectrum. We approach this requirement through analysis of isotopically labeled propane. In cases where multiple positions contribute to a single fragment ion, procedures for deconvolving their relative abundance must be established.

We must establish a reference frame based on the assumed or (preferably) known site-specific carbon isotope composition of a standard. This turns out to be the greatest hurdle at present, and was not resolved to our complete satisfaction over the course of this study (though, in principle, it need only be solved once).

3.1. Selection of fragment ions to measure

$C_2H_4^+$ presents an obvious target for isotopic analysis because it is the second most abundant ion generated by electron bombardment ionization of propane. We chose it instead of $C_2H_5^+$ due to the relatively greater stability of the background near $C_2H_4^+$ (Fig. 2). The background species of mass 29 causing us to choose the less abundant ion is depleted in mass relative to the alkane fragment and is assumed to be N_2H^+ ion, and like other nitrogen derivative ions on the lower masses is not stable through time. The choice of a second fragment to measure is less obvious: the methyl fragment ions are low in abundance, but potentially provide a pure measurement of the terminal carbon position. Most of the propyl fragment ions, and the molecular ion, are more abundant but contain a 2:1 mixture of terminal and central position carbons. Choosing one of these (or, equivalently, a conventional $\delta^{13}C$ measurement of propane) tends to dilute the constraints on the site-specific fractionation, meaning analytical errors would be magnified when the difference between the terminal and central position is computed.

Analysis of the propagated errors associated with these options suggests they are roughly equivalent. However, two factors lead us to focus first on a methyl fragment as the second constraint: (1) we prefer making a complete analysis on the Ultra rather than combining one Ultra measurement with a conventional $\delta^{13}C$ value, because it avoids potential systematic errors associated with combining data from multiple methods and standards. (2), the methyl fragment ions are a minor but ubiquitous feature of the mass spectra of a wide variety of organic matter. Thus, by producing a method capable of studying propane, we may have effectively met many of the technical requirements for position-specific analysis of other compounds. And, (3) the mass resolution needed to separate the relevant species scales with the fragment mass, and so is threefold more stringent for propyl than for methyl ions. Here we present data for both the CH_3^+ ion (the most abundant methyl fragment and therefore the obvious choice) and the CH_2^+ ion (a less obvious choice, but, as it happens, preferable due to common interferences by NH_n species). Finally, we present measurements of the full molecular ion for a subset of samples examined here, both as a test of analytical accuracy and as an alternative method that may be desirable in cases where the methyl fragment measurement is unusually difficult (e.g., due to the presence of an isobaric interference, or a contaminant that anomalously changes the fractionation behavior of the methyl fragment but seems to leave the propyl ions un-effected). Data regarding the abundance of different species and instrument configuration is shown in Table 1, as well as further discussed in the Supplemental material.

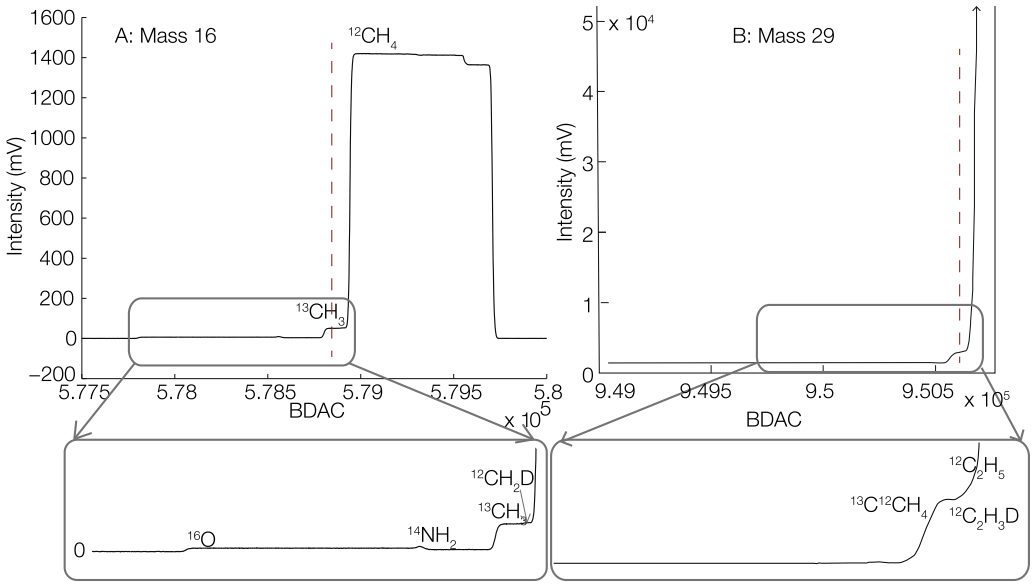

Fig. 2. (a and b) Mass spectrum illustrating representative analyte peaks and adjacent nearly-isobaric interferences for the $^{13}CH_3$ (left) and $^{13}C^{12}CH_4$ (right) species. The horizontal BDAC scale is proportional to mass. The mass 29 peak appears to be a small, possibly rounded shoulder, but it is statistically flat across a ~10 BDAC units width and thus is easily measured at high resolution (typical instrument stability is equivalent to ±1 BDAC unit over an hour).

Table 1
Configurations used to measure various species of interest, including cardinal mass of ion, cup number, detector type (numbers indicate the amplifier used to read a faraday cup), and typical measured voltages (for faradays) or counts per second, and equivalent currents.

Mass	Cup	Cup Location	Detector	mV or cps	fA
14	2	55.7	1.E+12	550	550
15	5	–	SEM	34,000	5.4468
15(old)	3	49.33	1.E+12	1050	1050
16	5	–	SEM	75,500	12.0951
28	4	25.33	1.E+11	1900	19,000
29	5	–	1.E+12	430	430
44	4	17.623	1.E+11	1100	11,000
45	5	–	1.E+12	360	360

4. RESULTS

4.1. Experimental constraints on fragmentation/recombination reactions

We studied the validity of our assumptions regarding which fragment ions sample which carbon sites by analysis of propane that was a physical mixture of natural propane (i.e., with a natural abundance of ^{13}C and D) and propane that had been artificially labeled in ^{13}C in one of its terminal carbon positions (i.e., $^{13}CH_3{}^{12}CH_2{}^{12}CH_3$). This labeled propane was added in systematically varying amounts to the reference gas and the mixtures then measured. If no exchange of carbon within or between propane molecules occurred during mixing and gas handling (something we consider implausible), and if the production of methyl and ethyl fragment ions follows our assumptions summarized in Eqs. (1)–(4), then the slope in a plot of ^{13}C enrichment for the methyl fragment versus that for the ethyl fragment should be 0.502, for any modest mixing ratio of labeled propane in natural propane. We observe a slope of 0.54 when all points are included (including a mixture with 500‰ enrichment in the methyl ion fragment). However, this result may be influenced by inaccuracies and non-linearities in our measurements of highly enriched gases. A slope of 0.51 is found when we consider only those mixtures that had $\delta^{13}C$ values for the methyl fragment ion within 120‰ of the reference gas (Fig. 4). We conclude that there is minor (~2–8%; most likely in the lower end of this range) mixing of center position carbon into the methyl fragment ion and/or excess terminal position carbon into the ethyl fragment ion during ionization. This is broadly similar to the extent of fragmentation/recombination involved in mass spectrometric analysis of the site-specific ^{15}N content of N_2O (Toyoda and Yoshida, 1999; Yoshida and Toyoda, 2000; Westley et al., 2007) or the clumped isotope analysis of CO_2 (Huntington et al., 2009; Dennis et al., 2011). We conclude that our method can potentially

recover at least relative differences (i.e., as compared to a reference standard (CIT-P1)) in the site-specific ^{13}C content of propane with only modest homogenization of methyl and methylene positions. Currently, we do not correct any of the data for this effect. The majority of the samples we have analyzed are within ~10‰ of our standard in both methyl and ethyl fragment composition, so corrections would be on the order of 0.2‰, which is similar to or smaller than our typical analytical error. In the future, if we study samples that differ markedly in site-specific carbon isotope composition from our standard, or if analytical precision improves significantly, say, to 0.1‰ or better, it may become important to correct the data for fragmentation/recombination artifacts. At this time, we believe it is more straightforward to present the data in the uncorrected form.

4.2. Sample measurement method

Measurements of unknown samples are standardized by comparison to a reference gas (described below). Each acquisition consists of 8 cycles of sample/standard comparison, with integration times of 16 s per cycle on each gas. One analysis of each fragment molecular ion species (i.e., one of the methyl fragments, or ethyl or propyl) is typically the average of four or five acquisitions, i.e., a total of 8–10 acquisitions are needed to calculate the difference in site-specific ^{13}C enrichment between the sample and reference gas based on analysis of two fragments, and an additional 4–5 acquisitions are needed to gather redundant information from the third species.

4.3. Standardization

One challenge to developing a new measurement of a previously un-studied isotopic property is establishing a reference frame that can be used to track long-term precision, report differences in composition between samples, and (in the event that this method is adopted elsewhere) compare data across labs. To this end, we obtained a tank of 99% grade propane from Air–Liquide and designated it as our intralaboratory reference tank. Its bulk carbon isotope ratio (averaged across all carbon positions) was measured by GC-online combustion IRMS in the laboratories of the PEER Institute, yielding a $\delta^{13}C_{PDB} = -33.23 \pm 0.55‰$.

In principle, it should be possible for us to constrain the absolute site-specific ^{13}C content of our reference gas based on the results of our mixing experiments; i.e., these mixtures provide a kind of 'standard additions' experiment that constrains the abundance of the terminally-substituted propane isotopologue in the standard into which labeled propane was mixed. However, propagation of the error in independently known mixing ratios of the natural and labeled end members (i.e., from manometry) shows that this constraint offers no meaningful (per mil level) determination of the difference in $\delta^{13}C$ between the central and terminal carbons in the reference gas.

Therefore, we currently report all data for unknown samples in a reference frame in which our intralaboratory standard (CIT-P1) is defined to be the '0' point on the $\delta^{13}C$ scale for both the central and terminal position $\delta^{13}C$ scales. This implies the following nomenclature:

$$\delta^{13}C_{center}{}^{CIT-P1} = \left(R^{13}{}_{center}{}^{sample}/R^{13}{}_{center}{}^{CIT\text{-}P1} - 1\right) \quad (5)$$

$$\delta^{13}C_{terminal}{}^{CIT\text{-}P1} = \left(R^{13}{}_{terminal}{}^{sample}/R^{13}{}_{terminal}{}^{CIT\text{-}P1} - 1\right) \quad (6)$$

where Eqs. (5) and (6) and the sample/reference gas comparisons of the methyl, ethyl and/or full molecular ions made during each analysis are combined to calculate $R^{13}{}_{i}{}^{sample}/R^{13}{}_{i}{}^{standard}$.

This approach does not differ in any fundamental way from the commonly-used reference frames for reporting stable isotope data (PDB, SMOW, etc.). However, it is unsatisfying because it prevents direct and unambiguous comparison of measured variations in site-specific isotopic differences with theoretical predictions or other methods that might differ in their analytical artifacts. Furthermore, it would be preferable to have our calibration tied to one of the internationally recognized reference frames, i.e. the V-PDB scale for carbon isotopes. For these reasons, we are currently working on alternative methods for determining the absolute distribution of isotopes within the standard based on selective chemical degradation (Gilbert et al., 2016) and/or NMR analysis (Gilbert et al., 2013) of our reference gas. These attempts have not yet succeeded, but when they do we anticipate that it should be straightforward to re-calculate all previously generated data to the V-PDB reference scale.

4.4. Measurement precision

We performed a series of measurements to document the precision of our methods and their conformance to expectations for physically simple, readily predicted fractionations.

The shot noise or counting statistical limit for each measurement can be calculated directly from the given source pressure and typical useful ion yield of the spectrometer. Typically, the limit for a methyl fragment acquisition of 8 cycles is 0.6‰ given the number of counts collected for the ^{13}C-bearing species on the SEM. The standard errors of the means for individual measurements, based on in-run stability (i.e., observed variation in the ratio from cycle to cycle), is between 0.8‰ and 0.6‰. For the ethyl fragment measurement, the shot noise limit is around 0.05–0.075‰ depending on source pressure and tuning conditions, and the typical external error for a measurement is closer to 0.1‰ (Fig. 3). For the propyl (full molecular ion) measurement, the shot noise is 0.05‰, and the in-run statistics are approximately the same. The reason why measurements of the propyl fragment achieves the shot-noise limit and the others do not may be related to the size of the flat peak on which the signal is integrated. When the source pressure decreases through time on the other measurements, this leads to a subtle shift in peak position (Eiler et al., 2013), which potentially has a greater effect on measurements of small 'shoulders' of peaks than on larger flat peak tops, since there is only a window of approximately 10 BDAC units (the magnetic step size) where the relevant signal can be stably measured.

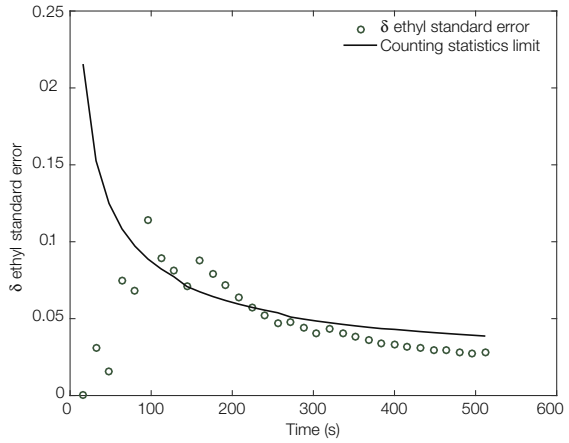

Fig. 3. Shows the relationship between counting time for the 2-carbon ethyl measurement, and the counting statistics limit. Average cumulative measurement time is for entire length of figure. Therefore the counting statistics limit is typically reached.

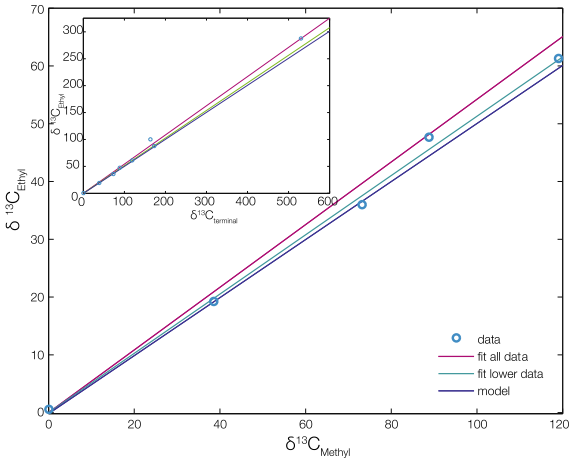

Fig. 4. Result of measurements of aliquots of propane reference standard mixed with variable amounts of $^{13}CH_3$—$^{12}CH_2$—$^{12}CH_3$. The 'model' line indicates the expectations under the assumptions expressed in Eqs. (1)–(5). The data suggest that fragmentation/recombination effects lead to several per cent deviation from this expectation, similar to broadly similar mass spectrometric methods for CO_2 and N_2O. Measurements of samples that are within ~120‰ of the standard in their methyl isotope ratio define a 'scrambling' fraction of only ~2%—almost indistinguishable from 0 and insignificant compared to typical analytical errors. The inset shows all data including the very enriched data point at 500‰ methyl value. This point has significant leverage on the fit, and is very far from the standard therefore the blue fit line is the preferred estimate of recombination during the measurement. (For interpretation of the references to color in this figure legend, the reader is referred to the web version of this article.)

To test external reproducibility, we analyzed replicates of samples. At the beginning of each session, after the collectors are aligned, two 'zero enrichment' measurements (i.e., comparison of the aliquot of the standard being used that day to a second aliquot of that same standard) are run for each of the fragments that are examined by the measurement. The average of a set of zero enrichments are within one standard deviation of zero. We also replicated some of the analyses of propane from Potiguar basin natural gases (below). These samples have been extracted from a container of natural gas at different times, cleaned of other gases separately, and then analyzed separately (generally as part of different sessions separated by weeks or months). Thus, these measurements test the experimental reproducibility of all elements of our measurement, at least for gases similar in composition to these 'wet' thermogenic natural gases. Most replicates of each fragment ion exhibit reproducibility similar to the 1-sigma standard error of one measurement (Table 2).

4.5. Tests of accuracy by comparison with conventional $\delta^{13}C$ values

We can test the accuracy of the method we present by comparing differences in calculated bulk $\delta^{13}C$ of the full propane molecule between two or more samples (i.e., based on measured differences in compositions of the methyl and ethyl fragment ions, in the CIT-P1 reference frame; Eq. (2)) to independently measured differences in $\delta^{13}C$ between aliquots of those same samples measured by conventional techniques in another laboratory. We choose for this purpose a suite of representative natural gases recovered from production wells in the Potiguar basin, Brazil, and analyzed for the $\delta^{13}C$ of propane at the PETROBRAS Research and Development Center (CENPES). The bulk $\delta^{13}C$ values calculated from our measurements of methyl and ethyl fragment ions are well correlated with independently known, conventional $\delta^{13}C$ values, with a slope indistinguishable from 1.0 ($r^2 = 0.849$), and an intercept of −0.5 that we interpret as arising from a difference in standardization between the two laboratories (Fig. 5; this discrepancy in standardization appears common to us based on several intercomparisons we have made with GC-IRMS analyses of n-alkanes; (Clog and Eiler, 2014; Stolper et al., 2014a,b)). This comparison suggests that our method accurately reproduces sample-sample differences in bulk $\delta^{13}C$, and thus (barring fortuitous cancelations of errors) that our measured variations in methyl and ethyl fragment ions accurately sample variations in central and terminal carbon positions. A geological interpretation of the site-specific carbon isotope variations among these natural gases will be presented in a future paper, along with a broader survey of natural gases and propane from laboratory pyrolysis experiments.

5. DISCUSSION

In this section we discuss the expected systematics of site-specific carbon isotope variations in propane for a variety of processes that may be relevant to natural systems. Our primary intention is to lay out a framework for future applied studies, but we also present some data that test the simpler of those predictions.

Table 2
Analytical results and dependent calculated site-specific isotopic compositions for the diffusion and mixing experiments and for the natural Potiguar Basin Suite. Dif label indicates sample that passed through the needle valve, whereas Res indicates sample remaining inside the glass bulb. Labels for mixing experiments are for sample reference only. Potiguar basin samples that have the same number, but a different modifier are replicates of the same bulk gas. The left set of columns present measurements of the terminal and two carbon fragments including standard deviation and standard error. The middle set of columns contain calculated values from those measured values using Eqs. (1)–(4) located in the text. For the Potiguar basin suite, the right columns are external conventional (GC-IRMS) data provided by the CENPES labs, Petrobras for the different hydrocarbon species present within the sample before being separated for propane.

Sample	Measurements						Calculations			External data				
	δ End	St dev	St err	δ Ethyl	St dev	St err	δ End	δ Center	δ Full	$\delta^{13}C\ CH_4$	$\delta^{13}C\ C_2H_6$	$\delta^{13}C\ C_3H_8$	$\delta^{13}C\ nC_4H_{10}$	$\delta^{13}C\ iC_4H_{10}$
Diffusion experiments														
Dif_1	−3.21	1.99	0.35	−3.50	0.59	0.11	−3.21	−3.80	−3.41					
Dif_3	−3.32	1.90	0.34	−3.53	0.73	0.13	−3.32	−3.74	−3.46					
Res_1	2.34	2.82	0.58	1.60	0.40	0.07	2.34	0.86	1.85					
Res_3	1.52	1.85	0.34	1.27	0.59	0.10	1.52	1.01	1.35					
Mixing experiments														
Aa	163.35	2.28	0.30	100.16	0.28	0.04	163.35	36.96	121.22					
Ab	530.42	4.11	0.55	287.62	15.59	2.85	530.42	44.83	368.55					
B3	119.06	10.01	1.25	61.04	0.67	0.09	119.06	3.02	80.38					
B1	172.80	3.95	0.70	87.67	0.50	0.09	172.80	2.54	116.05					
C4	73.19	3.58	0.63	35.75	3.25	0.57	73.19	−1.69	48.23					
C1	88.83	3.44	0.54	47.43	0.36	0.06	88.83	6.03	61.23					
D4	38.58	3.54	0.47	19.00	0.96	0.13	38.58	−0.57	25.53					
Potiguar basin suite														
1	6.82	1.65	0.24	4.88	0.85	0.13	6.82	2.94	5.53	−40.79	−31.21	−29.29	−28.49	−27.94
01a	4.67	1.62	0.26	5.67	0.51	0.08	4.67	6.66	5.33	−40.79	−31.21	−29.29	−28.49	−27.94
02b	1.66	1.69	0.69	0.46	0.67	0.12	1.66	−0.74	0.86	−48.25	−38.01	−34.81	−33.75	−34.64
3	4.84	2.41	0.38	3.72	0.39	0.07	4.84	2.59	4.09	−47	−34.84	−32.26	−31.75	−33.52
3b	3.19	1.76	0.31	1.41	0.84	0.12	3.19	−0.37	2.00	−47	−34.84	−32.26	−31.75	−33.52
03a	4.58	1.11	0.24	0.41	1.42	0.25	4.58	−3.77	1.80	−47	−34.84	−32.26	−31.75	−33.52
4	4.55	1.92	0.34	4.29	0.51	0.09	4.65	3.94	4.41	−45.02	−32.61	−29.84	−29.4	−31.28
4	4.56	1.50	0.22	5.53	1.17	0.19	4.56	6.51	5.21	−45.02	−32.61	−29.84	−29.4	−31.28
04a	6.28	1.89	0.33	4.73	0.63	0.11	6.24	3.23	5.23	−45.02	−32.61	−29.84	−29.4	−31.28
07a	0.76	2.96	0.52	0.05	0.38	0.29	0.76	−0.67	0.28	−47.14	−36.79	−34.27	−33.51	−34.53
7m	0.17	2.68	0.42	−0.22	0.61	0.11	0.17	−0.60	−0.09	−47.14	−36.79	−34.27	−33.51	−34.53
9	3.53	0.82	0.17	1.64	1.17	0.21	3.53	−0.24	2.27	−44.19	−32.87	−30.68	−30.87	−31.65

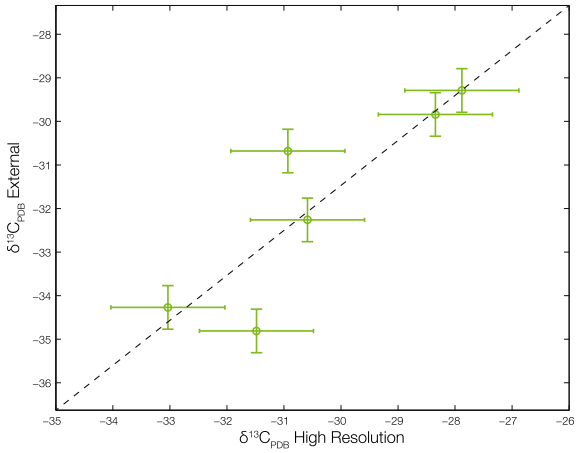

Fig. 5. Plot of bulk molecular $\delta^{13}C$ value of representative natural samples calculated from our measurements of methyl and ethyl fragment ions (horizontal axis) versus those measured independently by GC-combustion—IRMS (vertical error bars assume an estimated ±0.5‰ for these external measurements).

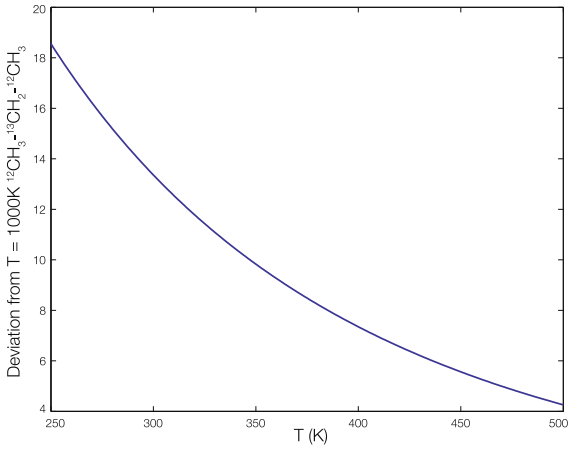

Fig. 6. Predicted relationship between the enrichment in ^{13}C in the center position of propane relative to the terminal positions (vertical axis, units are 1000.lnkeq for Reaction (7)) and temperature (horizontal axis, in kelvin). Equilibrium isotope effects tend to concentrate ^{13}C in the central position, by ~5–15‰ over geologically relevant temperatures, with a temperature sensitivity that may be suitable for geothermometry.

5.1. Homogeneous isotope exchange

We do not know *a priori* whether natural propane will commonly achieve internal isotopic equilibrium with respect to its various isotopologues. Nor did we succeed in producing an experimentally bracketed equilibrium as part of this study. Nevertheless, it is useful to estimate the direction, magnitude, and temperature dependence of isotopic variations driven by such exchange reactions, as a guide to interpreting the variations that may be observed in natural samples.

The quantum mechanical model of site-specific ^{13}C distribution in propane summarized below was first presented in Piasecki et al., 2015. Briefly, this study used density functional theory (DFT) to estimate the frequencies of fundamental vibrational modes for gaseous propane and the frequency shifts and free energy changes associated with ^{13}C substitution in the center or terminal carbon positions. These data are used to estimate the equilibrium constant for the reaction:

$$^{13}CH_3{}^{12}CH_2{}^{12}CH_3 \leftrightarrow {}^{12}CH_3{}^{13}CH_2{}^{12}CH_3 \quad (7)$$

The results indicate that for propane, as with most small molecules that have been studied for geochemical purposes (Wang et al., 2004; Ma et al., 2008), it is energetically favorable to partition the heavy isotopologues into sites and/or multiply-substituted combinations where their substitution will lead to the greatest reduction in the total vibrational enthalpy for an ensemble of molecules (Bigeleisen and Mayer, 1947; Urey, 1947). Fig. 6 shows the predicted deviation of the equilibrium constant for this reaction, in parts per thousand, from the high temperature limit of that equilibrium constant, plotted as a function of temperature (Piasecki et al., 2015). The results show that minimization of vibrational energy favors partitioning ^{13}C into the center position of propane. The effect is quite large at low temperature (19‰ at 250 K), and remains significant (~5–12‰) over geologically relevant temperatures. The amplitude and temperature variations of this predicted equilibrium effect should be easily resolved given the precision of our site-specific measurements (which result in an external error of ~1‰ for the difference in $\delta^{13}C$ between the terminal and central carbon positions).

There are, however, reasons to suspect that the equilibrium effects described above are unlikely to be manifest in natural propane. The majority of propane on earth is formed via the thermal degradation of larger organic molecules during burial, through reactions that are generally considered to be irreversible and thus should exhibit kinetic isotope effects rather than equilibrium ones (see below). It is less clear what to expect of less common pathways for propane formation, like Fischer–Tropsch synthesis (McCollom and Seewald, 2006) or biological synthesis (Hinrichs et al., 2006). It is conceivable that one or more of these propane synthesis pathways might equilibrate the carbon isotope structure of propane. And, perhaps even more familiar 'cracking' reactions could result in internally equilibrated propane if they occur in the presence of catalysts. If these cases exist and can be recognized, this effect could serve as a usefully precise geothermometer. It also seems likely that similar phenomena exist in larger molecules, and may be suitable for future study with methods related to those used here.

5.2. Diffusive fractionations

Diffusion of molecules through an aperture or some medium can lead to isotopic fractionations. When molecules diffuse through liquids or solids, the resulting fractionations are generally low in amplitude and follow mass laws that are not easily predicted. However, gas phase diffusion, either Knudsen diffusion or interdiffusion through a gaseous medium, is often large in amplitude

(multiple per mil to tens of per mil) and can be predicted with confidence using the kinetic theory of gases.

Knudsen diffusion of gaseous propane (i.e., at sufficiently long mean free path that collisions with other molecules can be neglected) follows the square-root mass law ($\alpha_{diffusion} = [m/m']^{0.5}$), leading to the expectation that $\delta^{13}C$ of diffused propane will be 11.26‰ lower than its residue (calculated as $1000 \times \ln(\alpha)$; note that this may be enhanced by Rayleigh distillation effects or diminished by retro-diffusion). If propane diffuses through a gas medium, i.e., where molecule–molecule collisions are more frequent than escape, the resulting fractionation depends on the mean molecular mass of that gas medium. For the example of propane diffusing through itself (mean molecular mass of 44.09 amu), diffused gas is 5.60‰ lighter than the residue. Important for our purposes, these predictions are independent of the site of ^{13}C substitution (except in extreme cases where ^{13}C enrichment greatly exceeds that of common natural materials, in which case multiple substitutions become common and non-linearities emerge in the relationships between concentrations, ratios and delta values). Thus, we predict that diffusive fractionations of propane will be observed as equal changes in the $\delta^{13}C$ of central and terminal carbon positions. This expectation might be violated if propane does not behave as a classical point mass, which could be the case if its collisions with surfaces or other molecules involve non-elastic interactions.

To compare with these predictions, we conducted an experiment in which a 5 L glass bulb was filled with a low pressure of propane (1.7 kPa). At the exit of the glass bulb, separated by a needle valve, was a glass finger submerged in liquid nitrogen. Propane diffused through the needle valve for 30 min and was collected beyond the valve with an effective pressure of 0 Pa due to propane being completely condensed in liquid nitrogen (thus, retro-diffusion should be minimal). The change in pressure for the experiment is 24 Pa after 50 μmol of propane was frozen into the glass sample finger. This indicates that only about 1.5% of the reservoir was depleted, so distillation effects will be insignificant.

Based on the pressure and temperature of the bulb, the experimental sample was in the gas phase inter-diffusion regime, leading to a predicted fractionation factor ($\delta^{13}C_{CITP1}$ of diffused gas minus the residual gas in the bulb) of −5.60‰.

The diffused portion of gas that was frozen into the glass finger was measured for its site-specific carbon isotope composition, as was an aliquot from the residual gas remaining in the glass bulb. The results of two separate experiments of this type are shown in Fig. 7 and Table 2.

The experimental data are consistent with the predicted fractionation factor for gas phase inter-diffusion with a separation of 5.2‰ which is within error to 5.6‰. In addition, the terminal and central positions are fractionated by the same amount (within analytical error), indicating as expected that the diffusive fractionation depends only on molecular mass and not on the molecular location of the heavy-isotope substitution, at least under the conditions of these experiments.

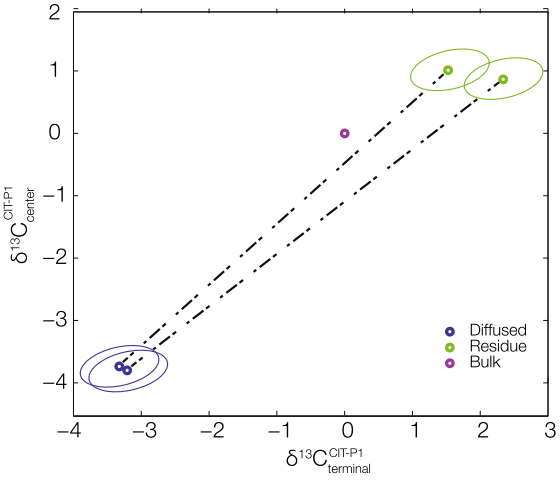

Fig. 7. Results of two diffusion experiments of propane through a needle valve. No site-specific preference was expected or measured, and the measured offset between the diffused gas and residue is within error of the expected value.

In both diffusion experiments, we observed a small but statistically significant difference of ~0.5‰ between the weighted average $\delta^{13}C$ values of the diffused and residual gas vs. that of the starting gas. We suspect that this is because the aliquots of gas used for each experiment were taken from the same large pressurized gas cylinder as the standard, but at a much later date. The gas cylinder is at high enough pressure that much of the propane is in liquid form, so removal of aliquots involves a phase transformation that may be isotopically fractionating. Thus, we suspect that the large gas cylinder has fractionated approximately 0.5‰ from its initial isotopic composition. The aliquot that we use as a daily working standard was taken from the cylinder approximately 1 year prior to these experiments, and is stored at below atmospheric pressure to insure that it is in the gas phase and not fractionated when aliquots are extracted (at least, by recognized processes).

It is worth considering whether other molecules, or propane at other conditions (e.g., very high pressure, or in the presence of a reactive medium), might exhibit fractionations that differ from the kinetic theory of gases due to chemical or physical phenomena. It is imaginable that hindered rotations or electrostatic and chemical interactions, for example, could lead to site-specific isotope effects in diffusion. This possibility is an attractive target for future research.

Finally, we note that we are not formally able to evaluate the accuracy of our measurements, because no standards of known (position-specific) composition exist. Nevertheless, the close agreement between predictions based on the kinetic theory of gases and our experimental results suggests that the measurements are nearly as accurate as they are precise.

5.3. Mixing

It is well known that clumped isotope compositions of molecular gases can exhibit relatively large anomalies

(i.e., differences from random proportions of multiply substituted isotopologues) simply due to mixing of samples that differ in bulk isotopic composition, even when the end members are similar in their proportions of clumped isotope species. These effects arise because (in the simple case of multiple substitutions of the same element) the random probability of forming a doubly substituted species goes as the square of the concentration of the rare isotope in question, and so is nonlinear. Thus mixing of heavy-isotope rich and heavy-isotope poor end members should generally result in mixtures that contain more doubly substituted species than would be present for a random isotopic distribution. This effect is well established for CO_2, O_2, CH_4, N_2O, C_2H_6 and has been explored in theory for H_2 (Eiler, 2007).

Although somewhat counterintuitive, in extreme cases similar effects can exist for site-specific isotopic fractionations (e.g., difference in $\delta^{13}C$ between the terminal and central position of propane). For example, subtle changes in site-specific fractionation should be introduced by mixing end members that differ in total molecular ^{13}C content provided at least one of the end members is very ^{13}C-rich; this occurs both because of non-linearities in the probabilities of multiple substitutions, and because isotope ratios do not have a perfectly linear dependence on concentrations of isotopologues. Nevertheless, our exploration of these issues through model calculations (Piasecki et al., 2015) suggests they lead to changes in site-specific carbon isotope fractionation in propane that are on the order of 0.01 per mil for most common cases, and thus are insignificant for our purposes. We suggest that they can be ignored, at least for propane having a natural abundance of ^{13}C.

5.4. Chemical-kinetic fractionations

Most natural propane is believed to form through catagenetic 'cracking' reactions that decompose sedimentary organic matter and release more volatile hydrocarbons. While the precise mechanisms of these reactions are not well known, general schemes, or families of related reactions, have been subject to extensive study and are better understood; see Xiao (2000) and references therein for a comprehensive review of this topic.

Previous studies that have considered the stable isotope systematics of propane formation through catagenesis assume (whether implicitly or explicitly), that the relevant reactions involve breaking a single C—C bond in a substrate compound to abstract a 3-carbon moiety, irreversibly and without re-ordering of carbon atoms from the parent molecule. If this is correct, propane should inherit the pre-existing carbon isotope structure of the precursors—kerogen constituents, bitumen, or oil—from which it forms, altered by kinetic isotope effects associated with C—C bond rupture (Chung et al., 1988; Tang et al., 2000).

Our understanding of the isotopic structure of kerogen and the kinetic isotope effects associated with propane formation is too crude to make a confident prediction of the resulting site-specific isotopic structures of natural propane molecules. Nevertheless, predictions arise naturally from adopting the assumptions of previous models of the bulk isotope fractionations (i.e., changes in $\delta^{13}C$) associated with catagenetic reactions, informed (where possible) by prior studies of the carbon isotope structures of organic compounds that could be propane precursors. Below we develop four such models. The first three models disregard variations in the isotopic structures of propane precursors (which are generally neglected in models such as Chung et al., 1988 and Tang et al., 2000) and focus on the kinetic isotope effects associated with 'cracking'. The fourth model considers recently published constraints on the carbon isotope structures of large hydrocarbons (Gilbert et al., 2013).

We begin with a simple and widely-used model for the interpretation of $\delta^{13}C$ values of n-alkanes in natural gases (Chung et al., 1988). This model assumes a starting reservoir of kerogen with a single $\delta^{13}C_{kerogen}$ value (assumed to be uniform at the molecular scale), and a fractionation (ε), equal to the $\delta^{13}C$ of kerogen minus the $\delta^{13}C$ of carbon abstracted from that kerogen by breaking a carbon—carbon bond (generally taken to be about 20‰, though likely a function of reaction temperature). In the simplest form of the Chung et al. model, ε is assumed to be both constant over time, and the same for reactions that form all highly volatile alkanes (methane, ethane, propane and butane) (Chung et al., 1988). Given these assumptions, and adopting the approximation that $\delta^{13}C$ and ε values can be added and subtracted without error, the first methane derived from cracking the kerogen will have a $\delta^{13}C$ value equal to $\delta^{13}C_{kerogen} - \varepsilon$. The first ethane formed will have initial $\delta^{13}C$ equal to $\delta^{13}C_{kerogen} - \frac{1}{2} \times \varepsilon$, because the fractionation only influences the carbon adjacent to the cleaved bond, not the other carbon (i.e. the effect is diluted by one-half). Similarly, the $\delta^{13}C$ of the first propane formed will be $\delta^{13}C_{kerogen} - \frac{1}{3} \times \varepsilon$. The Chung model does not assume any site-specific preference of the fractionation; nor does it necessarily have to state which of the carbons in product propane (terminal or central) is acted on by the fractionation. However, Chung et al. (1988) illustrate their model (Fig. 1 of that paper) as a family of n-alkanes that form by breaking the bond between what will become one of the terminal carbons of propane and the rest of its precursor molecule. In this case, the implication is that one of the two terminal sites of propane will be effected by ε, (such that the average of the two will be $\frac{1}{2}\ \varepsilon$), and the center position will be unfractionated. Thus, the expected trajectory linking reactant to product in a plot of central position $\delta^{13}C$ vs. terminal position $\delta^{13}C$ should be a horizontal line (Fig. 8a). And, increasing temperature or the effects of distillation on further reaction progress will move product propane back toward the reactant kerogen with increasing maturity (dashed 'hopping' path in Fig. 8a).

Second, we consider predictions that derive from the work of Tang et al., 2000, which presents quantum mechanical models for the kinetic isotope effects associated with reactions that are suggested to be representative of the production of volatile alkanes from larger precursor compounds. The Tang et al. model represents precursors as n-octadecane, which is cleaved at a C—C bond to generate methane, ethane, or propane. Their model predicts that the $\delta^{13}C$ of propane produced by this process, averaged across all sites, will be 9‰ lower than its precursor (which

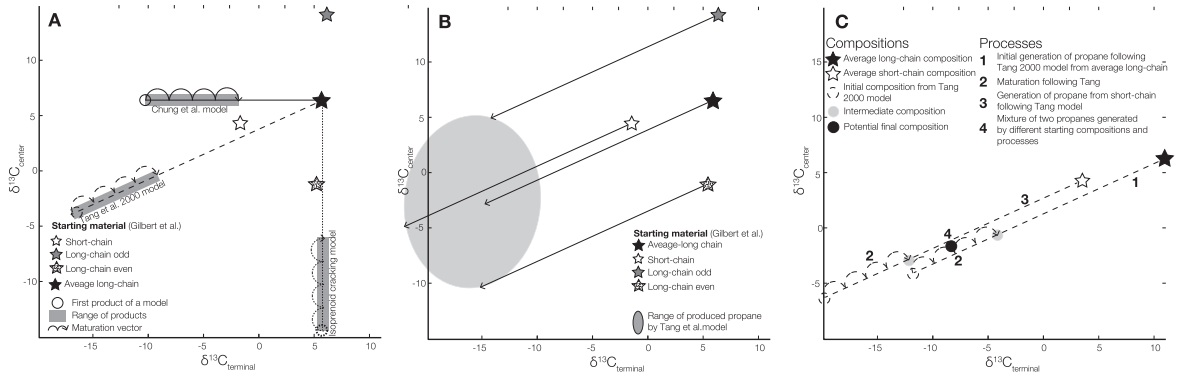

Fig. 8. (a–c) Expected site-specific fractionations from idealized models of catagenetic reactions that produce propane. Different vectors in part A reflect different previously published fractionations as applied to large organic molecules that could potentially produce propane. Part B shows the range of initial propanes that could be generated following the Tang et al. path from Part A. The different starting compositions represent a range of internal structures of long chain alkanes measured by NMR. Part C integrates a theoretical sequence of events that could form a final propane molecule present within the rock record, from initial generation from two different larger organic molecule, maturation following the Tang et al., 2000 model, and finally a mixture between the propanes produced from two different starting compositions.

is again taken to be isotopically homogeneous), at a reaction temperature of 500 K (where their calculations best match experimental data). This atomistic, first-principles model permits prediction of isotope effects associated with ^{13}C substitution in all three of the carbons that will be transferred to product propane: The fractionation, ε, associated with the carbon adjacent to the cleaved bond (one of the two carbons that will occupy terminal positions in product propane) is 19‰, whereas that for the center position is 5‰, and the distal terminal fractionation is only 3‰ (again, all calculated at 500 K). Thus, the average fractionation for terminal carbons in propane is 11‰, whereas that for the center carbon is 5‰. And so, the fractionation predicted by this model results in a vector linking product to reactant having a slope near ø in Fig. 8a, rather than the horizontal trajectory predicted by the simpler Chung et al. model. Again, increasing maturity (temperature and/or reaction progress) should produce a trend of increasing $\delta^{13}C$ of propane approaching the reactant.

Third, we consider the possible consequences of propane production from a precursor isoprenoid, where, unlike the n-alkanes considered in the previous two models, the atom adjacent to the bond being cleaved becomes the central position in product propane. In this case, we would expect the isotope effect associated with propane forming reactions to most influence the center position, and have little or no effect on terminal positions (which would express only secondary isotope effects). We are not aware of any previous effort to construct a first-principles model that predicts the kinetic isotope effects associated with such a reaction, and constructing such a model is beyond the scope of this study. However, we can consider the first-order results of such a process by assuming a fractionation similar to that predicted by Tang for C—C cleavage to release propane as a product (19‰ at 500 K), and simply assume this applies to the central carbon position with negligible fractionations on the adjacent terminal positions. This leads to a predicted vector linking product propane to reactant kerogen in Fig. 8a that is vertical—orthogonal to that predicted based on the Chung et al. model—and relatively high in amplitude (because the fractionation is not diluted by mixing with relatively unfractionated sites, as occurs for the terminal carbon position).

Finally, we consider the possible effects of carbon isotope heterogeneity in the precursor compounds on the carbon isotope structure of product propane. Gilbert et al. (2013) report contrasts in $\delta^{13}C$ between the terminal three carbon positions of C11 through C29 n-alkanes. The samples have no geologic context and the measurements made in this study constrain only relative differences in $\delta^{13}C$ among the terminal 3 carbon sites, but not differences relative to other sites or the bulk molecule; nevertheless, this is the only study to examine site-specific carbon isotope distributions in large hydrocarbons. The samples conform to one of three patterns: short chain alkanes (C11—C15) have no contrast between the C2 and C3 positions, but low $\delta^{13}C$ 'ends' (C1 position; on average ~12‰ lighter than C2 or C3); longer chain n-alkanes having even carbon numbers (C16, C18, etc.), have C1 positions that are ~10–12‰ higher in $\delta^{13}C$ than C2 positions, which are similar to or lower than C3 positions (~0–5‰ contrast); and longer chain, odd-carbon-number compounds (C17, C19, etc.) have C1 positions somewhat lower than C2 (~0–5‰, though C17 is an exception), and C2 positions that are much higher than C3 (10–18‰).

One more assumption is needed before we can make use of the data from this study: the absolute $\delta^{13}C$ of any one site. We suggest that a plausible initial hypothesis is that most of the 'action' in this data set is controlled by isotopic variations near the tips of the studied molecules (because this is where primary isotope effects are more likely to have acted during any prior bond cleaving reactions). On this basis, we speculate that the C3 positions of these compounds are most similar to one another. We assume that the final three positions of all of the starting alkanes follow the pattern following Gilbert et al., and that these n-alkanes will yield propane by breaking the C3—C4 bond (i.e., following Chung et al., 1988 and Tang et al., 2000). Therefore we illustrate the range of compositions that might arise due to differences in isotopic structure among substrates

(Fig. 8a). When looking at this figure, one should imagine a set of possible fractionations resembling the vectors described above, emanating from each of the various possible substrate isotope structures. Fig. 8b shows the range of possible initial propanes that could be produced by applying the Tang et al. (2000) model of fractionation to the three major classes of alkane precursor structure reported by Gilbert et al. (2013). And finally, Fig. 8c shows one of several possible scenarios in which a range of propane isotopic compositions are generated in a single system both by varying the progress of the cracking reaction, and by changing relative proportions of precursors that differ from one another in isotopic structure.

Taken together, the preceding discussion suggests a wide range of isotopic patterns may characterize the production of propane from irreversible 'cracking' of precursor kerogen or petroleum compounds, ranging from ~10–20 per mil effects on the terminal carbon to similar effects on the central carbon, or combinations of these two extremes. However we can organize these variations into two end member effects: central position variations seem best attributed to changes in the molecular or isotopic structure of the precursor (i.e., n-alkane vs. isoprenoid; long vs. short chain isotope structure), whereas terminal position variations seem most sensitive to the factors that modulate the precursor-propane fractionation (temperature and reaction progress). Thus, while this subject is too poorly understood to yield confident *a priori* predictions about the site-specific composition of natural propane, any observations we make can potentially lead us to favor one or another of these models as hypothesized mechanisms of propane formation.

6. CONCLUSIONS

We present a method for measuring differences in site-specific carbon isotope fractionation in purified propane based on high-resolution isotope ratio mass spectrometry of two or more fragment ions in the mass spectrum of the intact molecule. Typical precision and accuracy for site-specific $\delta^{13}C$ are 0.5–1.0‰ for samples containing 50 μmol propane. The same approach should be generalizable to many other volatile organic molecules, providing a route to exploring the multi-dimensional isotopic anatomy of organic molecules. The method we present requires significantly less sample material than NMR techniques (~50 μmols vs. ~10 mmols); thus, mass spectrometric techniques may be an avenue to expanding the study of site specific carbon isotope variations to the relatively small samples commonly available to environmental and geochemical studies.

The application of the method we present to natural propane is described in a forthcoming companion paper. However, we note here that existing models for the generation of propane from 'cracking' of kerogen, bitumen and oil compounds imply that the mechanisms and progress of these reactions should result in multiple-per-mil variations in the site-specific carbon isotope composition of propane (Chung et al., 1988; Tang et al., 2005). And, in the unlikely case that natural propane reaches thermodynamic equilibrium (e.g., through highly reversible reactions), theoretical models predict that its site specific carbon isotope content could be used as a geothermometer (Webb and Miller, 2014; Piasecki et al., 2015).

ACKNOWLEDGEMENTS

This work was funded by an NSF-EAR instruments and facilities grant. Additional funding was supplied by Exxon Mobil and Petrobras. I would also like to thank the reviewers including Prof. Shuhei Ono for their helpful comments to make the manuscript more clear and precise.

APPENDIX A. SUPPLEMENTARY DATA

Supplementary data associated with this article can be found, in the online version, at http://dx.doi.org/10.1016/j.gca.2016.04.048.

REFERENCES

Abelson P. H. and Hoering T. C. (1961) Carbon isotope fractionation in the formation of amino acids by photosynthetic organisms. *Proc. Natl. Acad. Sci. U.S.A.* **47**, 623.

Berner U., Faber E., Scheeder G. and Panten D. (1995) Primary cracking of algal and landplant kerogens: kinetic models of isotope variations in methane, ethane and propane. *Chem. Geol.* **126**, 233–245.

Bigeleisen J. and Mayer M. G. (1947) Calculation of equilibrium constants for isotopic exchange reactions. *J. Chem. Phys.* **15**, 261.

Caer V., Trierweiler M., Martin G. J. and Martin M. L. (1991) Determination of site-specific carbon isotope ratios at natural abundance by carbon-13 nuclear magnetic resonance spectroscopy. *Anal. Chem.* **63**, 2306–2313.

Caytan E., Botosoa E. P., Silvestre V., Robins R. J., Akoka S. and Remaud G. S. (2007) Accurate quantitative ^{13}C NMR spectroscopy: repeatability over time of site-specific ^{13}C isotope ratio determination. *Anal. Chem.* **79**, 8266–8269.

Chung H. M., Gormly J. R. and Squires R. M. (1988) Origin of gaseous hydrocarbons in subsurface environments: theoretical considerations of carbon isotope distribution. *Chem. Geol.* **71**, 97–104.

Clayton C. (1991) Carbon isotope fractionation during natural gas generation from kerogen. *Mar. Pet. Geol.* **8**, 232–240.

Clog M. and Eiler J. (2014) *C—H and C—C Clumping in Ethane by High-Resolution Mass Spectrometry*. American Geophysical Union Abstract.

Clog M., Eiler J., Guzzo J. V. P., Moraes E. T. and Souza I. V. A. (2013) Doubly ^{13}C-substituted ethane. *Mineral. Mag.* **77**, 805–933.

DeNiro M. J. and Epstein S. (1977) Mechanism of carbon isotope fractionation associated with lipid synthesis. *Science* **197**, 261–263.

Dennis K. J., Affek H. P., Passey B. H., Schrag D. P. and Eiler J. (2011) Defining an absolute reference frame for "clumped" isotope studies of CO. *Geochim. Cosmochim. Acta* **75**, 7117–7131.

Eiler J. (2007) "Clumped-isotope" geochemistry—the study of naturally-occurring, multiply-substituted isotopologues. *Earth Planet. Sci. Lett.* **262**, 309–327.

Eiler J., Clog M., Magyar P., Piasecki A., Sessions A. L., Stolper D., Deerberg M., Schlueter H.-J. and Schwieters J. (2013) A high-resolution gas-source isotope ratio mass spectrometer. *Int. J. Mass Spectrom.* **335**, 45–56.

Gilbert A., Yamada K. and Yoshida N. (2013) Exploration of intramolecular ^{13}C isotope distribution in long chain n-alkanes (C_{11}—C_{31}) using isotopic ^{13}C NMR. *Org. Geochem.* **62**, 56–61.

Gilbert A., Yamada K., Suda K., Ueno Y. and Yoshida N. (2016) Measurement of position-specific ^{13}C isotopic composition of propane at the nanomole level. *Geochim. Cosmochim. Acta* **177**, 205–216.

Hinrichs K. U., Hayes J. M., Bach W., Spivack A. J., Hmelo L. R., Holm N. G., Johnson C. G. and Sylva S. P. (2006) Biological formation of ethane and propane in the deep marine subsurface. *Proc. Natl. Acad. Sci. U.S.A.* **103**, 14684–14689.

Huntington K. W., Eiler J., Affek H. P., Guo W., Bonifacie M., Yeung L. Y., Thiagarajan N., Passey B., Tripati A., Daëron M. and Came R. (2009) Methods and limitations of "clumped" CO_2 isotope (Δ 47) analysis by gas-source isotope ratio mass spectrometry. *J. Mass Spectrom.* **44**, 1318–1329.

Lamprecht G. and Pichlmayer F. (1994) Determination of the authenticity of vanilla extracts by stable isotope ratio analysis and component analysis by HPLC. *J. Agric. Food Chem.* **42**, 1722–1727.

Ma Q., Wu S. and Tang Y. (2008) Formation and abundance of doubly-substituted methane isotopologues ($^{13}CH_3D$) in natural gas systems. *Geochim. Cosmochim. Acta* **72**, 5446–5456. http://dx.doi.org/10.1016/j.gca.2008.08.014.

Macko S. A., Fogel M. L., Hare P. E. and Hoering T. C. (1987) Isotopic fractionation of nitrogen and carbon in the synthesis of amino acids by microorganisms. *Chem. Geol. Isot. Geosci. Sect.* **5**, 79–92.

Magyar P., Kopf S., Orphan V. and Eiler J. (2012) Measurement of nitrous oxide isotopologues and isotopomers by the MAT 253 Ultra. *Mineral. Mag*.

Martin G. J., Zhang B. L. and Naulet N. (1986) Deuterium transfer in the bioconversion of glucose to ethanol studied by specific labeling at the natural abundance level. *J. Am. Chem. Soc.* **108**, 5116–5122.

McCollom T. M. and Seewald J. S. (2006) Carbon isotope composition of organic compounds produced by abiotic synthesis under hydrothermal conditions. *Earth Planet. Sci. Lett*.

Monson K. D. and Hayes J. M. (1980) Biosynthetic control of the natural abundance of carbon 13 at specific positions within fatty acids in Escherichia coli. Evidence regarding the coupling of fatty acid and phospholipid synthesis. *J. Biol. Chem.* **255**, 11435–11441.

Monson K. D. and Hayes J. M. (1982) Carbon isotopic fractionation in the biosynthesis of bacterial fatty acids. Ozonolysis of unsaturated fatty acids as a means of determining the intramolecular distribution of carbon isotopes. *Geochim. Cosmochim. Acta* **46**, 139–149.

Moussa I., Naulet N. and Martin M. L. (1990) A site-specific and multielement approach to the determination of liquid-vapor isotope fractionation parameters: the case of alcohols. *J. Phys. Chem.* **94**, 8303–8309.

Ono S., Wang D. T., Gruen D. S., Sherwood Lollar B., Zahniser M. S., McManus B. J. and Nelson D. D. (2014) Measurement of a doubly substituted methane isotopologue, ^{13}CH 3D, by tunable infrared laser direct absorption spectroscopy. *Anal. Chem.* **86**, 6487–6494.

Piasecki A., Sessions A. L., Peterson B. and Eiler J. (2015) Prediction of equilibrium distributions of isotopologues for methane, ethane, and propane using density functional theory. *Geochim. Cosmochim. Acta*.

Rustad J. R. (2009) Ab initio calculation of the carbon isotope signatures of amino acids. *Org. Geochem.* **40**, 720–723. Available at: <http://linkinghub.elsevier.com/retrieve/pii/S0146638009000643>.

Schauble E. A., Ghosh P. and Eiler J. (2006) Preferential formation of ^{13}C–^{18}O bonds in carbonate minerals, estimated using first-principles lattice dynamics. *Geochim. Cosmochim. Acta* **70**, 2510–2529.

Singleton D. A. and Szymanski M. J. (1999) Simultaneous determination of intermolecular and intramolecular ^{13}C and ^{2}H kinetic isotope effects at natural abundance. *J. Am. Chem. Soc.* **121**, 9455–9456.

Snell K. E., Koch P. L., Druschke P., Foreman B. Z. and Eiler J. (2014) High elevation of the "Nevadaplano" during the Late Cretaceous. *Earth Planet. Sci. Lett.* **386**, 52–63.

Stolper D. A., Lawson M., Davis C. L., Ferreira A. A., Neto E. V. S., Ellis G. S., Lewan M. D., Martini A. M., Tang Y., Schoell M., Sessions A. L. and Eiler J. (2014a) Formation temperatures of thermogenic and biogenic methane. *Science* **344**, 1500–1503.

Stolper D. A., Sessions A. L., Ferreira A. A., Santos Neto E. V., Schimmelmann A., Shusta S. S., Valentine D. L. and Eiler J. (2014b) Combined ^{13}C-D and D-D clumping in methane: methods and preliminary results. *Geochim. Cosmochim. Acta* **126**, 169–191.

Stolper D. A., Martini A. M., Clog M., Douglas P. M., Shusta S. S., Valentine D. L., Sessions A. L. and Eiler J. (2015) Distinguishing and understanding thermogenic and biogenic sources of methane using multiply substituted isotopologues. *Geochim. Cosmochim. Acta*, 1–61.

Takenaka S., Kuriyama T., Tanaka T. and Funabiki T. (1995) Photooxidation of propane over alkali-ion-modified V_2O_5/SiO_2 catalysts. *J. Catal.* **155**, 196–203.

Tang Y., Perry J. K., Jenden P. D. and Schoell M. (2000) Mathematical modeling of stable carbon isotope ratios in natural gases. *Geochim. Cosmochim. Acta* **64**, 2673–2687.

Tang Y., Huang Y., Ellis G. S., Wang Y., Kralert P. G., Gillaizeau B., Ma Q. and Hwang R. (2005) A kinetic model for thermally induced hydrogen and carbon isotope fractionation of individual n-alkanes in crude oil. *Geochim. Cosmochim. Acta* **69**, 4505–4520.

Toyoda S. and Yoshida N. (1999) Determination of nitrogen isotopomers of nitrous oxide on a modified isotope ratio mass spectrometer. *Anal. Chem.* **71**, 4711–4718.

Uehara K., Yamamoto K., Kikugawa T. and Yoshida N. (2003) Site-selective nitrogen isotopic ratio measurement of nitrous oxide using 2 μm diode lasers. *Spectrochim. Acta Part A Mol. Biomol. Spectrosc.* **59**, 957–962.

Urey H. C. (1947) The thermodynamic properties of isotopic substances. *J. Chem. Soc.*, 562–581.

Wang Z., Schauble E. A. and Eiler J. (2004) Equilibrium thermodynamics of multiply substituted isotopologues of molecular gases. *Geochim. Cosmochim. Acta* **68**, 4779–4797. Available at: <http://linkinghub.elsevier.com/retrieve/pii/S001670370400451X>.

Webb M. A. and Miller, III, T. F. (2014) Position-specific and clumped stable isotope studies: comparison of the Urey and path-integral approaches for carbon dioxide, nitrous oxide, methane, and propane. *J. Phys. Chem.* **118**, 467–474. Available at: <http://pubs.acs.org/doi/abs/10.1021/jp411134v>.

Westley M. B., Popp B. N. and Rust T. M. (2007) The calibration of the intramolecular nitrogen isotope distribution in nitrous oxide measured by isotope ratio mass spectrometry. *Rapid Commun. Mass Spectrom.* **21**, 391–405.

Xiao Y. (2000) Modeling petroleum and natural gas generation. In *Molecular modeling theory: applications in the geosciences. Reviews in Mineralogy and Geochemistry*, vol. 42, pp. 383–436.

Yeung L. Y., Ash J. L. and Young E. D. (2014) Rapid photochemical equilibration of isotope bond ordering in O_2. *J. Geophys. Res. Atmos.*, n/a–n/a.

Yoshida N. and Toyoda S. (2000) Constraining the atmospheric N_2O budget from intramolecular site preference in N_2O isotopomers. *Nature* **405**, 330–334.

Associate editor: Jochen J. Brocks